Joint inference of CFC lifetimes and banks suggests previously unidentified emissions

Megan Lickley (mlickley@mit.edu)
Massachusetts Institute of Technology https://orcid.org/0000-0001-5810-8784
Sarah Fletcher
Stanford University
Matt Rigby
University of Bristol https://orcid.org/0000-0002-2020-9253
Susan Solomon
Massachusetts Institute of Technology https://orcid.org/0000-0002-2020-7581

Article

Keywords: Chlorofluorocarbons, inferred emissions, CFC lifetimes

Posted Date: August 17th, 2020

DOI: https://doi.org/10.21203/rs.3.rs-53675/v1

Version of Record: A version of this preprint was published at Nature Communications on May 18th, 2021. See the published version at https://doi.org/10.1038/s41467-021-23229-2.

Joint inference of CFC lifetimes and banks suggests previously unidentified emissions

Authors: Megan Lickley[1*], Sarah Fletcher[2], Matt Rigby[3] and Susan Solomon[1]

1. Department of Earth, Atmospheric, and Planetary Sciences, Massachusetts Institute of Technology, Cambridge, MA 02139, USA.
2. Civil and Environmental Engineering, Stanford University, Stanford, CA, 94305, USA
3. School of Chemistry, University of Bristol, Bristol, BS8 1QU, UK

* corresponding author: mlickley@mit.edu

Abstract

Chlorofluorocarbons (CFCs) are harmful ozone depleting substances and greenhouse gases. CFC production was phased-out under the Montreal Protocol, however recent studies suggest new and unexpected emissions of CFC-11. Quantifying CFC emissions requires accurate estimates of both atmospheric lifetimes and ongoing emissions from old equipment (i.e. 'banks'). In a Bayesian framework we simultaneously infer lifetimes, banks and emissions of CFC-11, 12 and 113 using available constraints. We find that lifetimes of all three gases are likely shorter than previous estimates, suggesting that best estimates of inferred emissions are larger than recent evaluations. Our analysis indicates that bank emissions are decreasing faster than inferred emissions, and we estimate new,

unexpected emissions during 2014-2016 were 19.6, 16.2, and 7.7 Gg/yr for CFC-11, 12 and 113, respectively. While recent studies have focused on unexpected CFC-11 emissions, our results call for further investigation of potential sources of emissions of CFC-12 and CFC-113, along with CFC-11.

Introduction

The Montreal Protocol entered into force in 1989 and led to the phase-out of industrial production of nearly all ozone depleting substances (ODSs) by 2010. This global action reduced emissions of ODSs and avoided massive worldwide ozone losses[1]. There are now signs that the Antarctic ozone "hole" is beginning to heal[2,3]. While the phase-out of ODSs has led to decreases in their atmospheric abundance, recent studies have pointed to an observed and unexpected delay in the decrease of CFC-11 concentrations, indicating ongoing emissions of this gas that may be linked to illicit production[4,5]. CFC-11 is the most abundant source of chlorine in the atmosphere and a potent greenhouse gas. Limiting its production and emissions is therefore critical both for ozone recovery and to safeguard the planet against climate change. Quantifying illicit emissions of CFCs has been limited by uncertainties in their underlying emissions from old equipment (i.e. "banks") with uncertain leak rates (release fractions), as well as the lifetimes of these molecules in the atmosphere. Joint consideration of atmospheric lifetimes together with observed changes in atmospheric concentrations hence provide our best estimate of global total emissions (i.e. both bank and illicit emissions). Earlier work has focused on quantifying the size of CFC banks and potential contributions to future emissions[6]; here

48 we focus on jointly estimating lifetimes of CFC-11, 12 and 113 as well as the magnitude
49 and sources of global emissions of these gases using all available information in a
50 probabilistic framework.
51
52 While there are several lifetime estimation methods, (e.g. tracer-tracer or observation-
53 based methods, see SPARC[7] for details), two of the most widely used techniques are
54 discussed here. The first makes use of 3D chemical climate models (CCM) that integrate
55 chemical sink loss frequencies and calculated global distributions[8]. Results from six 3D
56 CCMs and one 2D CCM were made available through the Stratosphere-troposphere
57 Processes and their Role in the Climate (SPARC) modeling effort[9,7], a project of the
58 World Climate Research Program. Observations of surface concentrations are generally
59 used only as a qualitative check in such calculations, which largely depend on the
60 modeled transport and chemistry. The second approach infers lifetimes in a Bayesian
61 framework using near-surface mole fraction measurements and, typically, fixed estimates
62 of emissions as inputs to an atmospheric model[10]. These different approaches have led to
63 wide ranges in estimated lifetimes (see Table 1), and therefore large differences in
64 inferred emissions (Chapter 6 of SPARC[7]).
65
66 While knowledge of atmospheric lifetimes allows for emissions to be inferred from
67 changes in observed concentrations, further analysis is required to partition the source of
68 those emissions from new production versus emissions from banks. The former would
69 represent a breach of the Montreal Protocol while the latter remains permitted at this
70 time, highlighting the policy importance of quantifying bank emissions. There are

various approaches to quantifying banks and their emissions. A "top-down" approach makes use of observationally-derived emissions along with assumptions regarding production and lifetimes[11]. The size of banks are then estimated as the cumulative difference in production and emissions over time.

Some emissions, such as leakage during production, occur quickly (here referred to as direct emissions), while some is delayed by storage in banks. Figure 1 illustrates how small differences in lifetime and production assumptions can propagate into large differences in top-down inferred banks. Figure 1 further illustrates how small differences in assumed bank release fractions (i.e., leakage rate from banks) can propagate into uncertainties in the source of emissions (i.e. whether emissions come from banks versus direct emissions from new production). Figure 1 serves to illustrate how different seemingly reasonable assumptions about lifetimes, production, and release fractions can both match observed concentrations and lead to very different conclusions about the quantity and sources of emissions, with some combinations of assumptions being unphysical (i.e. producing negative direct emissions). Further examples are presented in the SI.

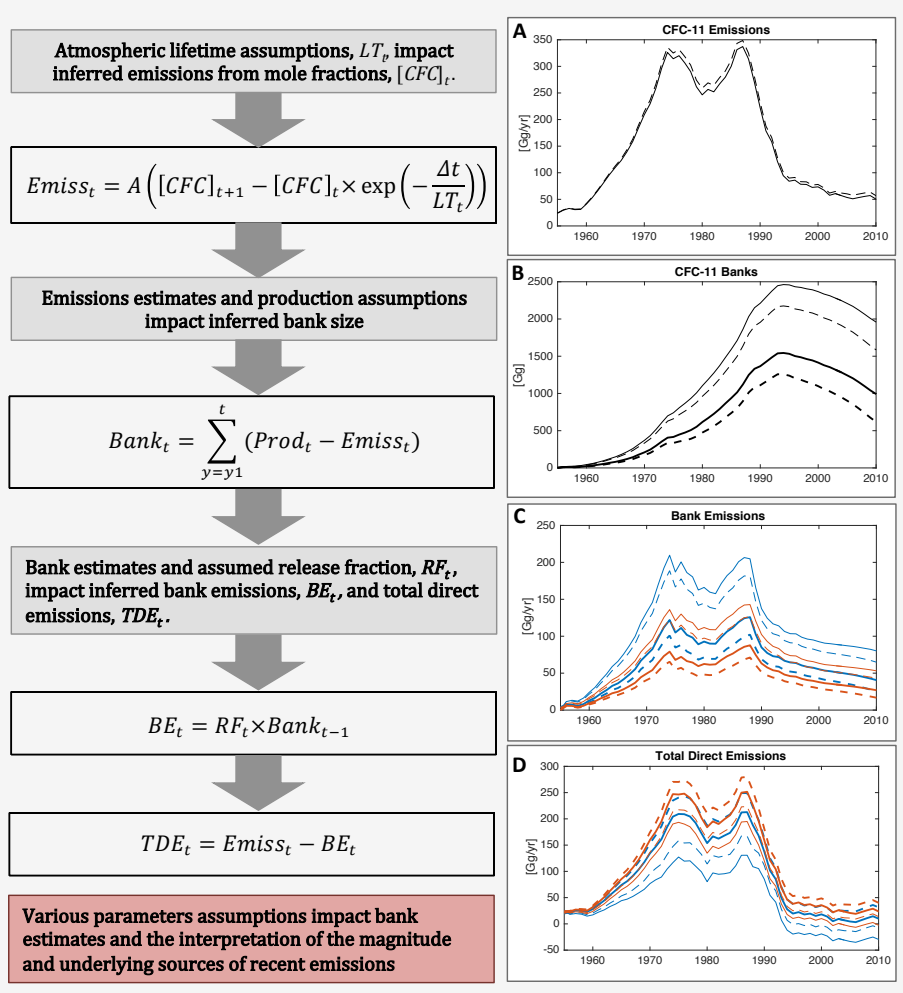

Figure 1: Diagram of the impacts of parameter assumptions including lifetime (LT) on inferred total emissions (Emiss) obtained from observed concentrations, as well as bank size (Bank), bank emissions (RF×Bank) and total direct emissions (TDE). Panel A illustrates the impacts of two lifetime assumptions on inferred total emissions, while Panels B-D provide illustrative examples to show the sensitivities of the breakdown of sources of those emissions to components from banks versus direct emissions. The solid lines throughout correspond to quantities derived assuming the SPARC multi-model mean time-varying lifetime, and the dashed lines correspond to an assumed constant lifetime of 52 years, adopted as

the steady state lifetime in the work of Rigby and colleagues[5] and WMO (2018)[3]. Panel A shows the emissions estimate using the first equation. The parameter, A, is a constant that converts units of atmospheric concentrations to units of emissions. Panel B shows the bank estimates for the two lifetime scenarios and two illustrative production scenarios; bank estimates using reported production are shown using the thicker lines, and the thinner lines correspond to a production scenario that is 10% larger than reported. Panel C shows inferred bank emissions for the lifetime scenarios and production scenarios described above. The colors of the lines indicate different bank release fraction estimates. Blue lines correspond to bank emissions for the median of the prior release fractions distributions used in the analysis from this paper. The red lines correspond to the median $+1\sigma$ of the prior release fraction distribution. Panel D shows the broad range of resulting inferred direct emissions, with the lines corresponding to the same scenarios used in Panel C.

An alternative "bottom-up" approach to estimating banks and their emissions makes use of industry reported production data along with a careful tallying of multiple equipment types and estimated release fractions over time[12,13]. While this approach is less reliant on indirect inference of bank magnitudes than the top-down approach, it requires accurate and complete reporting and does not make full use of all available data, such as atmospheric observations.

In recent work, Lickley and colleagues[6] take a Bayesian Parameter Estimation (BPE)

approach which makes use of observationally-derived emissions to apply inference to a deterministic bottom-up bank simulation model on a gas-by-gas basis for CFC-11, 12, and 113. This bank estimation approach incorporates the widest range of constraints to date, including observations, reported production data, and previously published release rates partitioned by equipment types and their respective uncertainties. That work found banks of CFC-11 and 12 were likely larger than previous scientific assessments suggested, although CFC-11 banks alone could not account for the recent uptick in global emissions that Montzka and colleagues[4] inferred from observed concentrations.

An important limitation of the BPE model was in the treatment of atmospheric lifetimes. Rather than inferring lifetimes from the BPE model, Lickley and colleagues[6] considered several atmospheric lifetime scenarios to estimate their role in quantifying banks and their contributions to future emissions. Here, we extend the BPE model from Lickley et al. (2020)[6] to jointly rather than individually infer lifetimes and their uncertainties for CFC-11, 12 and 113 and address correlations across molecules. This is done using SPARC CCM modeled lifetimes to construct joint lifetime priors for CFC-11, 12 and 113 that reflect the lifetime uncertainties and correlations both across time and gases in the BPE model. The lifetimes of CFC-11, 12 and 113 are dependent on atmospheric transport and related chemical loss processes, so are considered correlated with each other. Evidence of correlated lifetimes comes, for example, from the SPARC set of models, where a model producing lower than average CFC-11 lifetimes also produces lower than average CFC-12 and 113 lifetimes. Adding these new constraints to the BPE model allows us to simultaneously infer lifetimes along with total emissions, bank size, and

bank emissions over time. In this way, we can better quantify and partition recent emissions into bank emissions versus unexpected sources using all available information.

Results

To derive lifetimes, emissions and their respective sources, we build on the Bayesian Parameter Estimation approach to modeling banks and emissions developed by Lickley and colleagues[6]. The basic framework develops a bottom-up simulation model that simultaneously models banks, emissions (partitioned into bank emissions versus direct emissions), and mole fractions over time. The simulation model relies on inputs including reported production of each equipment type, estimates of release fractions and their respective uncertainties, and lifetime estimates developed using the SPARC CCM values. We develop prior distributions for each of the input parameters using previously published values, including jointly modeled priors for CFC-11, 12 and 113 lifetimes. Sampling from these prior distributions, we also develop priors for each of the outputs of the simulation model (i.e. banks, bank emissions, direct emissions and mole fractions). Observed mole fractions are treated as observations in Bayes' Theorem and used to estimate the posteriors of each of the inputs and outputs of the simulation model (See Methods for more details).

Figure 2 shows the observations, prior and posterior distributions of mole fraction estimates for CFC-11, 12 and 113. The observations are within the range of inferred posterior model predictions of the data for all gases throughout the whole time period

(1955-2010). Posterior residuals (i.e. $\boldsymbol{D}_j - M_j$ from eq (8); see Methods) are shown in the supplement (Fig S1) and appear normally distributed around zero.

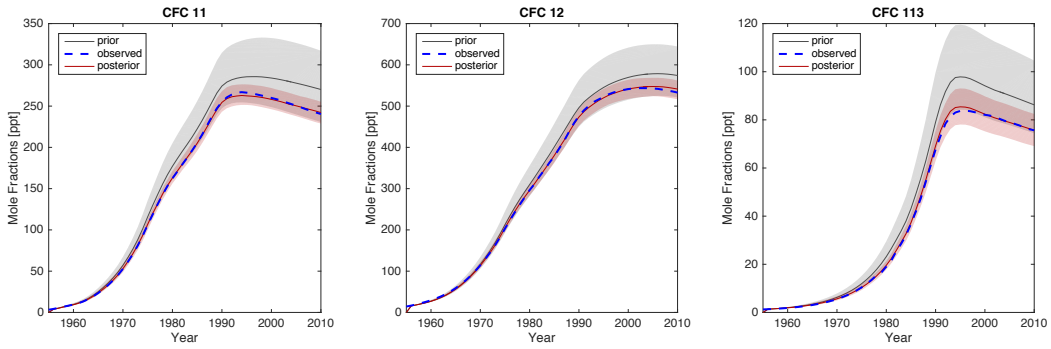

Figure 2: Mole fraction estimates. The grey line and shaded region indicate median and 95% CI of the prior distribution for each molecule. The dashed blue lines are observed concentrations and the red line and shaded region indicate the median and 95% CI for the posterior distributions.

Figure 3 shows prior and posterior emissions estimates, calculated using the parameter-based estimate of emissions (i.e. eq 2; see Methods), compared to an observationally-derived estimate, where emissions are inferred using mole fractions and atmospheric lifetimes (i.e. solving for $E_{j,t}$ using eq 1 of Methods). This provides a useful contrast to previous emissions comparisons from Lickley et al. (2020)[6], which adopted both a time-varying lifetime and constant scenario equal to the SPARC multi-model mean. Compared to Lickley et al. (2020), the posterior emissions in Figure 2 show a closer match between parameter-based and observationally derived emissions as well as lower uncertainties, which can be explained in part by lifetimes being inferred instead of

assumed. By jointly inferring lifetimes, observationally-derived emissions are represented as a distribution instead of fixed values, and our simulated emissions and mole fractions are assumed to have lower uncertainty than in the Lickley et al. (2020), where lifetimes were fixed. This leads to a smaller posterior distribution in parameter-based emissions estimates that more closely matches the observationally-derived estimates. We note that WMO 2018 emissions estimates for CFC-11 are within the uncertainty of posterior observationally-derived emissions. For CFC-12 and 113, however, WMO 2018 emissions fall below the range of posterior observationally-derived emissions towards the end of the simulation period, a result of posterior lifetimes being shorter for these two gases than what is assumed in WMO 2018[3].

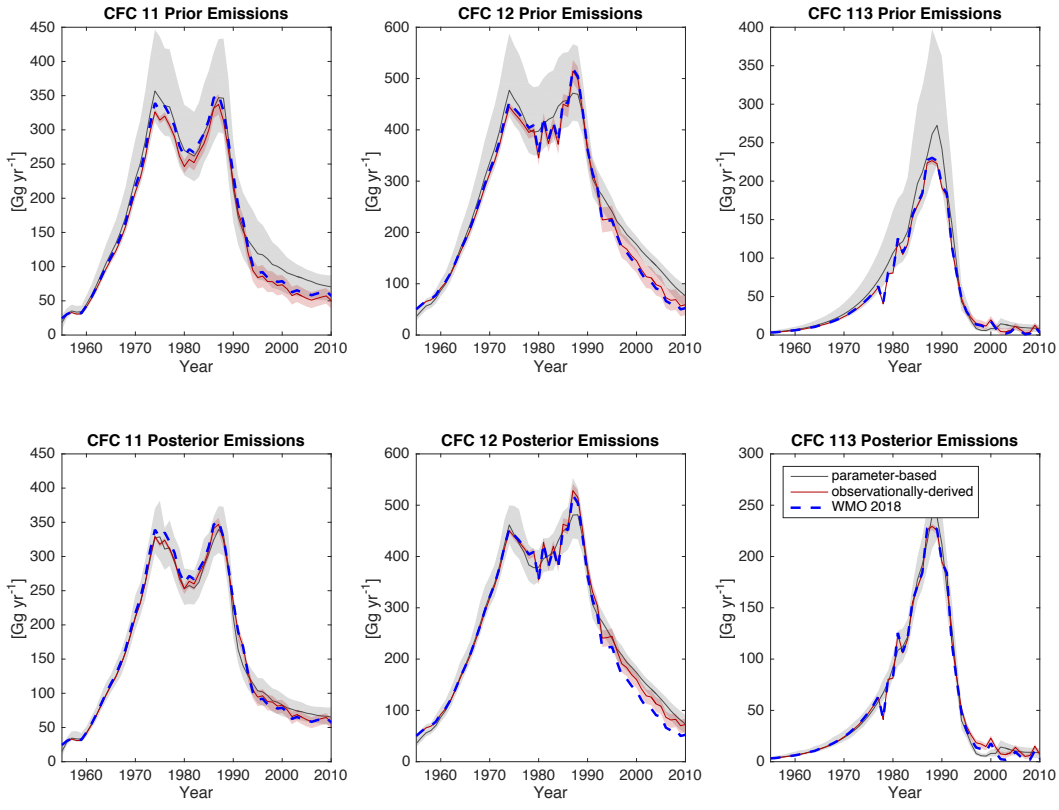

Figure 3: Emissions comparisons of observationally-derived (red) and parameter-based (grey) inferred emissions for the priors (top figures) and posteriors (bottom figures). The solid lines indicate the median and the shaded region indicates the 95% CI for both prior and posterior distributions. The uncertainties in observationally-derived emissions reflect the role of uncertainties in lifetimes and thus are updated in the posterior to reflect the lifetime posterior estimates.

Figure 4 shows the time-varying prior and posterior lifetime estimates for CFC-11, 12, and 113. The SPARC multi-model mean is included for comparison. This figure shows that the median joint posterior lifetime estimates are shorter than the SPARC multi-model mean values, though within the 2-sigma range, for all three species. Note that it is not surprising that similar differences with the posterior are found for all species, due to the strong correlation assumed between model lifetimes. If the BPE is instead run without assuming lifetime dependency across molecules, then the result looks substantially different (Figure S2). In this case, CFC-12 posterior lifetimes are significantly lower than the SPARC multi-model mean, whereas CFC-11 and CFC-113 posterior estimates are more similar to their priors than the joint posterior estimates. This finding shows that our results are strongly dependent upon the inclusion of model lifetime uncertainties that are highly correlated between species. This correlation is obtained from the SPARC model ensemble, reflecting that the lifetimes of CFC-11, 12 and 113 are governed by similar physical and chemical processes as noted above. Thus, we argue that its inclusion makes the best use of the available evidence. The uncorrelated version of the model

leads to a higher estimated lifetime and lower estimated DE for CFC-11, and thus higher banks. Considering the joint dependency across molecules, inferring lifetimes instead of assuming them, and therefore reducing the assumed variance in the likelihood function accounts for much of the difference between bank estimates found here and Lickley et al. (2020) (See Figure S3 and S4).

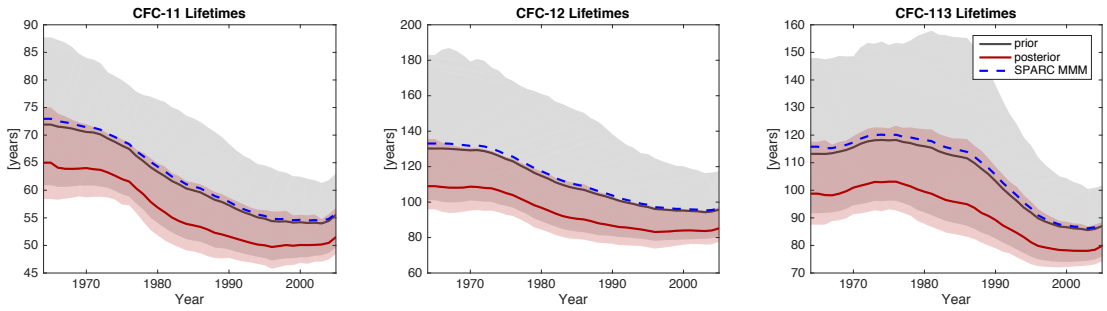

Figure 4: Time varying lifetime distributions. The black line and grey shaded region indicate the median and 95% CI of the prior lifetimes, derived from SPARC modeled values. The dashed blue line indicates the SPARC multi-model mean. The red line and shaded region indicate the median and 95% CI of the posterior lifetime distributions.

The posterior time-averaged lifetime estimates and 2010 lifetime estimates are shown in Table 1 along with comparisons with previously published estimates. While our CFC-11 lifetime estimates agree with the SPARC recommended lifetime estimates, our CFC-12 and 113 estimates are outside the 2-sigma range that SPARC estimated to be "most likely" (shown in Table 1), but within their "possible" 2-sigma range ((78, 151) for CFC-12 and (69, 138) for CFC-113; see Chapter 6 in SPARC[7]). We adopt the 2010 posterior lifetime distributions from our analysis, along with 2010 posterior distributions of Bank

and RF distributions to forward simulate observationally-derived total emissions for 2011 to 2016, Bank emissions, and their difference, which we refer to as Direct Total Emissions. This is done for inferred parameter distributions allowing both an unexpected emissions scenario (as in Lickley et al., 2020[6]) and reported emissions scenario in order to provide our best estimate of the sources and magnitude of emissions that can include unexpected production and release if suggested by all the inputs. However, for our post-2010 estimated values, we assume that RF remains constant and we do not account for a portion of further new production going into banks (since this is both poorly known and is expected to be relatively small compared to the existing bank). Results are shown in Figures 5 for the unexpected emission scenario and the reported production scenario is provided in Figure S5. Direct total emissions are shown in Figure 6.

Table 1: Posterior atmospheric lifetime estimates for the unexpected emissions scenario and a comparison with previously published estimates. Results shown from the present study include a 95% CI (p2.5, p97.5).

	Median Posterior for 2010 (p2.5, p97.5)	**Median time averaged lifetime (p2.5, p97.5)**	**WMO (2003)/ IPCC (2001)**	**SPARC recommended steady state ("most likely" 2-sigma CI)**	**Rigby et al. (2013) (1-sigma CI)**
CFC-11	51.5 (48.6, 56.6)	56.3 (52.3, 63.0)	45	52 (43, 67)	52 (45, 61)
CFC-12	85.2 (78.0, 97.3)	94.7 (83.6, 111.9)	100	102 (88, 122)	112 (95, 136)
CFC-113	79.9 (74.1, 88.4)	91.1 (82.5, 107.2)	85	93 (82, 109)	109 (97, 124)

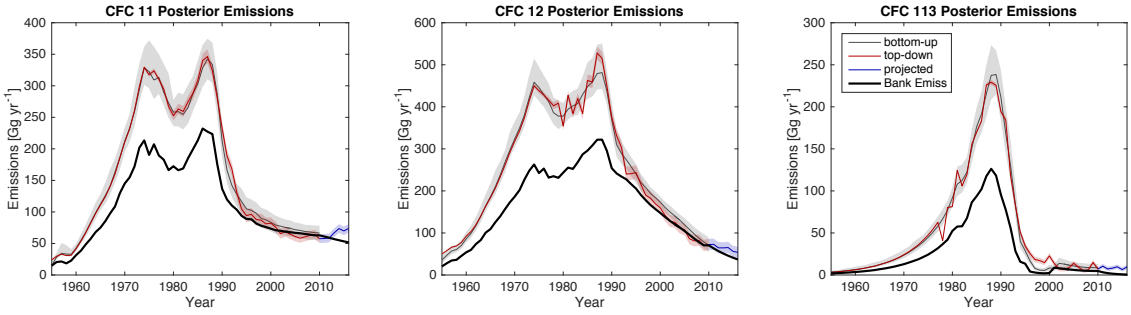

Figure 5: Posterior emissions (red and grey), median posterior bank emissions (black), observationally derived emissions with posterior lifetimes (blue). Shaded regions indicate the 95% confidence interval.

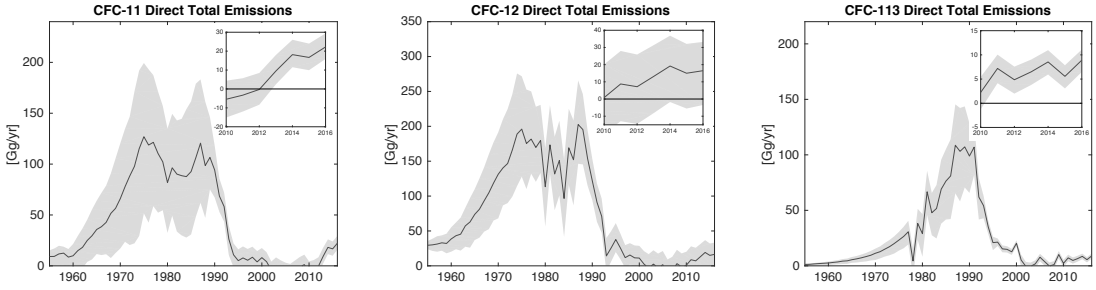

Figure 6: Direct total emissions (i.e. posterior top-down emissions minus bank emissions). Shaded region indicates the 95% confidence interval.

Table 2: Average emissions (95% CI) by source for the unexpected emission scenario. Values are reported in [Gg/yr]

	CFC-11	CFC-12	CFC-113

Bank Emissions 2002-2012	64.0 (53.1,75.2)	92.1 (73.4, 108.2)	5.4 (3.3, 8.2)
Total Emissions 2002-2012	62.2 (52.4, 68.9)	91.5 (76.0, 103.3)	8.8 (5.9, 11.1)
Direct Total Emissions 2002-2012	-2.1 (-12.1, 8.3)	-0.1 (-22.6, 18.3)	3.4 (-0.8, 6.8)
Bank Emissions 2014-2016	52.9 (45.4, 61.1)	43.0 (27.7, 61.1)	0.82 (0.08, 3.1)
Total Emissions 2014-2016	72.7 (63.7,78.7)	58.6 (43.7, 69.6)	8.6 (6.0, 10.8)
Direct Total Emissions 2014-2016	19.6 (9.2, 28.3)	16.2 (-7.5, 32.9)	7.7 (3.8, 10.3)

Discussion and Conclusions

Table 2 summarizes the key findings of our study. In this analysis we set out to estimate lifetimes and their uncertainties for CFC-11, 12 and 113, and provide information on their emissions and sources of emissions. Our analysis suggests that the lifetime of CFC-11 is 51.5 years with a 95% CI of (48.6, 56.6), in the range of most previously estimated values. We estimate CFC-12 and CFC-113 lifetimes to be 85.2 years with a 95% CI of (78.0, 97.3), and 79.9 years with a 95% CI of (74.1, 88.4), respectively. Both mean values for CFC-12 and 113 estimated lifetimes are lower than previous surface mole fraction trend-based estimates[10], although they are statistically consistent, at the 2-sigma level, with SPARC 2013 "possible" ranges[7]. We attribute this difference in estimated values to the inclusion of a wider range of constraints in our analysis, namely the inclusion of co-dependencies across molecules' lifetimes. This is an important distinction between this work and previous publications, which did not account for such co-dependencies across molecules. The present study probabilistically accounts for the correlation in lifetimes across gases as exhibited by chemistry-climate models (from

296 SPARC). That is, shorter (longer) than average lifetimes for one gas will likely imply
297 shorter (longer) than average lifetimes for the other gases. Here we show that including
298 such dependencies clarifies our conclusions about lifetimes, as illustrated in Figure 4
299 versus Figure S2.
300
301 Montzka et al. (2018)[4] used a single set of NOAA observations along with a constant
302 lifetime of 57 years to estimate total CFC-11 emissions from 2002-2012 to be 54 Gg/yr,
303 and from 2014-2016 to be 67 Gg/yr, with an unexpected increase of 13±5 Gg/yr. Here
304 we use both the AGAGE and NOAA global observational datasets that are merged along
305 with other constraints to estimate average total CFC-11 emissions from 2002-2012 of
306 approximately 62.2 Gg/yr and from 2014-2016 of approximately 72.7 Gg/yr, with a
307 difference of 10.6 Gg/yr, and a 95% CI of (10.0, 11.3). Rigby et al. (2019) provided
308 evidence that an emission increase of 7 ± 3 Gg/yr occurred from eastern China between
309 the periods 2008 – 2012 and 2014 - 2017. We find that while a large fraction of total
310 emissions over these time periods does come from banks, significant decreases in bank
311 emissions as banks are depleted (see Table 2) suggests that a significant increase of direct
312 total emissions is occurring over time. Our best estimate of total direct emissions of
313 CFC-11 from 2014-2016 is 19.6 Gg/yr, with a 95% CI of (9.2, 28.3). Therefore, we find
314 that total unexpected emissions likely due to new production in breach of the Protocol is
315 likely to be higher than the increase inferred by Montzka et al. (2018)[4] by about 6.6
316 Gg/year. Further, our best estimate exceeds the contribution estimated for eastern China
317 by Rigby et al. (2019) by about 12.6 Gg/year, supporting the proposal that unexpected
318 sources elsewhere are likely (notwithstanding that Rigby et al, 2019 only estimated the

magnitude of the rise in emissions, rather than the excess over a declining bank, as we have in this work). However, the lower limit of our 95 percent confidence range is within Rigby et al. (2019)'s stated uncertainty range, indicating that it is unlikely but plausible that eastern China is the only source.

For CFC-12, emissions are consistently decreasing post-2000. Nonetheless, since our estimate of bank emissions are on average decreasing faster than total emissions, significant direct total emissions from 2014-2016 are also very likely to be occurring for this gas. CFC-12 direct emissions for 2014-2016 are estimated to be 16.2 Gg/yr, with uncertainties large enough to contain zero only at the 95% CI. Further, between 2002-2012 and 2014-2016 there is a significant *increase* in estimated direct emissions of 15.7 Gg/yr, with a 95% CI of (10.3, 20.3); i.e., exceedingly unlikely to include zero. This finding strongly merits further investigation, as CFC-12 production is expected to accompany CFC-11 production in most chemical plants[14]. Estimated total CFC-113 emissions are approximately 8. 8 Gg/yr with an approximate 95% CI of (6.0, 11.0) for both 2002-2012 and 2014-2016. Further, given the decrease in bank emissions, we estimate the direct total emissions to have increased to 7.7 Gg/yr in 2014-2016 from 3.4 Gg/yr in 2002-2012, substantially larger than expected from its allowed reported global use in feedstocks (see Lickley et al., 2020).

Overall, our findings strengthen the understanding of estimates and their uncertainties for lifetimes, banks, and apparent direct emissions of all three of the major CFCs, 11, 12, and 113. We have shown that all three molecules are likely being directly emitted in

342 comparable amounts between 2014 and 2016, in contrast to expectations under the
343 Montreal Protocol. Determining the sources of these emissions and whether and how to
344 reduce them is a pressing challenge for the Parties to the Montreal Protocol.
345
346
347 **Methods**
348
349 In this section, we discuss the adaptations to the BPE model developed in Lickley et al.
350 (2020). This model is implemented by first developing a bottom-up simulation model
351 for CFC-11, 12 and 113 that uses a collection of input parameters to recursively simulate
352 outputs, which include mole fractions, $M_{j,t}$, emissions, $E_{j,t}$, and banks, $B_{j,t}$, for
353 molecule j, in year, t. The input parameters include atmospheric lifetimes, $\tau_{j,t}$,
354 production, $Prod_{j,t}$, direct emissions, $DE_{j,t}$, and bank release fractions $RF_{j,t}$. The
355 equations for the deterministic simulation model are shown in eqs (1) – (3). Mole
356 fractions are modeled as;

$$M_{j,t} = M_{j,t-1} \times \exp\left(\frac{1}{\tau_{j,t}}\right) + A \times E_{j,t} \quad (1)$$

357
358 where A is a constant that converts units of emissions to units of mole fractions. We
359 follow Daniel et al. (2007)[16] and let A include a fixed factor of 1.07 to account for the

360 increased mixing ratios at the surface relative to globally average values. Emissions,

361 $E_{j,t}$, in eq (1) are modeled as;

$$E_{j,t} = RF_{j,t} \times B_{j,t-1} + DE_{j,t} \times Prod_{j,t} \quad (2)$$

362 and banks, $B_{j,t,}$ in eq(2) are modeled recursively as

363

$$B_{j,t,} = (1 - RF_{j,t}) \times B_{j,t-1} + (1 - DE_{j,t}) \times Prod_{j,t} \quad (3)$$

364 Prior distributions for each of the input parameters are described below and in Lickley et

365 al. (2020). While the deterministic simulation model is independent across molecules,

366 chemistry-climate models demonstrate that the lifetimes of molecules exhibit

367 interdependencies across molecules. We therefore obtain joint posterior distributions of

368 the vector of input parameters by implementing Bayes' theorem as follows;

369

$$\begin{aligned} &P(\theta_{11}, \theta_{12}, \theta_{113} | D_{11}, D_{12}, D_{113}) \\ &\propto P(\theta_{11}, \theta_{12}, \theta_{113}) P(D_{11} | \theta_{11}, \theta_{12}, \theta_{113}) P(D_{12} | \theta_{11}, \theta_{12}, \theta_{113}) P(D_{113} | \theta_{11}, \theta_{12}, \theta_{113}), \end{aligned} \quad (4)$$

370

371 where θ_j's denote the vector of inputs and outputs of the deterministic simulation model

372 (eqs 1-3) and D_j denotes the data (i.e. observed mole fractions) for molecule, j. We

373 assume that the data (D_{11}, D_{12}, and D_{113}) are conditionally independent given

374 θ_{11}, θ_{12}, and θ_{113}. This assumption implies that the relationship between D_{11}, D_{12}, and

375 D_{113} is captured in the simulation model described in (1-3), but that the errors between
376 data and model are uncorrelated across molecules.
377
378 In eq (4), $P(\theta_{11}, \theta_{12}, \theta_{113})$ describes the joint prior distribution of the input parameters
379 and outputs for CFC-11, 12 and 113 for all model years. $P(D_j|\theta_{11}, \theta_{12}, \theta_{113})$ is the
380 multivariate likelihood of all years of observed mole fractions of molecule *j*, given the
381 parameters of the deterministic simulation model as described in eqs (1 - 3), i.e. the error
382 between data and simulation model. For computational efficiency, we solve eq (4) using
383 sequential Bayesian updating. To do so, we first solve for the posterior
384 $P(\theta_{11}, \theta_{12}, \theta_{113}|D_{11}, D_{12})$ where
385

$$P(\theta_{11}, \theta_{12}, \theta_{113}|D_{11}, D_{12}) \propto P(\theta_{11}, \theta_{12}, \theta_{113})P(D_{11}|\theta_{11}, \theta_{12}, \theta_{113})P(D_{12}|\theta_{11}, \theta_{12}, \theta_{113}) \quad (5)$$

386
387 This posterior is then used as the prior distribution and updated given observed mole
388 fractions of CFC-113 (D_{113}), obtaining a posterior distribution equivalent to eq (4);

$$P(\theta_{11}, \theta_{12}, \theta_{113}|D_{11}, D_{12}, D_{113}) \propto P(\theta_{11}, \theta_{12}, \theta_{113}|D_{11}, D_{12})P(D_{113}|\theta_{11}, \theta_{12}, \theta_{113}), \quad (6)$$

389 The posteriors in eqs (4 – 6) are obtained by multiplying by a normalizing constant such
390 that the right hand side integrates to 1.
391
392 To solve for the posterior in eq (4), the model is implemented as follows.

1. First develop prior distributions for all input parameters in $\boldsymbol{\theta}$. This includes joint prior distributions for τ_{11}, τ_{12} and τ_{113} as well as $Prod_{j,t}$, $DE_{j,t}$, and $RF_{j,t}$.
2. Using Monte Carlo simulation, sample from the prior distributions and simulate many realizations of mole fraction time series using equations (1), (2) and (3).
3. Specify likelihood function of observed mole fractions given simulated mole fractions (i.e. the error between data and model).
4. Estimate the joint posteriors of eq (5) and (6) using the sampling importance ratio method described further below.

We describe each step of the model in more detail below.

Prior Distributions

Release Fraction and Direct Emissions

For each molecule, priors are developed for release fraction (RF) and direct emissions (DE) using industry reported data and previously published emissions functions[12]. As in Lickley et al. (2020), we jointly estimate RF and DE priors using a bottom-up accounting method that evaluates the composition of the bank over time. This includes accounting for various equipment type and release fractions. RF is modeled as a fraction of the bank and depends on the type of equipment in the bank in any given year. DE is modeled as a fraction of production and depends on the type of equipment produced in a given year. An update since Lickley et al. (2020), is that the prior DE of foam now follows a beta distribution (with parameters 5, 5) centered at 1.5%, based on values reported in Ashford

(2004). For a detailed description of other RF and DE priors, see the Supplemental Information in Lickley et al. (2020).

Production

Production priors are modeled as in Lickley et al. (2020), where a lognormal distribution is assumed with a lower bound that is 95% of global reported values. Reported values of global production come from the Alternative Fluorocarbon Environmental Acceptability Study (AFEAS) for years prior to 1989, and from the United Nations Environmental Program (UNEP) from 1989 onwards. We adopt a correction for the AFEAS data following WMO (2002)[11] where AFEAS production values are augmented with production data from UNEP. We assume autocorrelation over time in the bias of reported production and infer this autocorrelation parameter (see Lickley et al. (2020) for more details). For CFC-113, we adjusted prior distributions so that observed mole fractions are contained in the prior simulated mole fraction range. This was achieved by setting a lower bound of production to 70% of reported and doubling the uncertainty range (i.e. changing B from 0.2 to 0.4, see Lickley et al. (2020) for details). We include two scenarios for production, one where the priors are based on reported production and one where both CFC-11 and CFC-113 have 'unexpected emissions' from 2000 onwards in line with estimates from Montzka et al. (2018) and Lickley et al. (2020). Since CFC-11, 12 and 113 are considered jointly, the method can also reveal whether unexpected production of CFC-12 is likely.

Lifetimes

We develop joint priors for the atmospheric lifetimes that take into account the correlation in lifetimes over time and across molecules. We develop priors for lifetimes using SPARC modeled values as follows:

1. Compute the inverse of each modeled lifetime (since the inverse of lifetimes typically assumed to be normally distributed, Chapter 6 of SPARC[7]). We then smooth the inverse lifetime using a 10-year moving average. Most modeling groups that contributed lifetime estimates to SPARC, considered the period from 1960 to 2010. Some available modeled lifetime calculations end before 2010, in which case we assume the last 10-year averaged value holds for the remainder of the time period.
2. For each molecule, j, create a $N_{yrs} \times N_{models}$ matrix, K_j, of the smoothed inverse lifetimes. N_{yrs} is equal to 42; the number of SPARC modeled years after smoothing with a 10-yr window. N_{models} is the number of SPARC models and is equal to 7.
3. We assume that the inverse of these modeled lifetimes are normally distributed, Our prior lifetime distributions are then modeled as;

$$\begin{matrix} 1/\tau_{11} \\ 1/\tau_{12} \\ 1/\tau_{113} \end{matrix} \sim N\begin{pmatrix} \mu_{11} \\ \mu_{12}\,, \Sigma^{\tau} \\ \mu_{113} \end{pmatrix}, \tag{7}$$

where μ_j is a $N_{yrs}\times 1$ vector equal to the row average of K_j and Σ^{τ}, is a $3N_{yrs}\times 3N_{yrs}$ matrix equal to the covariance of $\begin{bmatrix} K_{11} \\ K_{12} \\ K_{113} \end{bmatrix}$.

4. Samples from this prior will represent the inverse lifetimes from 1965 to 2006. Lifetime samples are extended on each end of the time series to obtain an estimated prior from 1955 to 2010 (i.e. the 1965 value in the sample is applied to all years prior to 1965, and the 2006 value is applied to all subsequent years).

Likelihood Functions

Likelihood of observed data given modeled mole fractions

Observed mole fractions come from the merged dataset based on AGAGE and NOAA global mean surface station measurements[17]. Data are available from 1980 to 2018. Due to large uncertainties in unreported emissions since 2012 and due to SPARC lifetime estimates ending in 2010, we base the likelihood of each simulation on yearly observed data between 1980 to 2010. We assume that;

$$\boldsymbol{D}_j = M_j + \boldsymbol{\epsilon_j}, \tag{8}$$

where $\boldsymbol{D}_j$ is a $N_{Obs}\times 1$ vector where N_{Obs} corresponds to 31 years and each input is yearly observed mole fractions for molecule, *j*, between 1980 and 2010. M_j is a $N_{Obs}\times 1$

vector of simulated mole fractions, accounting for dependence across all molecules, and $\boldsymbol{\epsilon_j}$ is a $N_{Obs}\times 1$ vector corresponding to the error term and is assumed to be normally distributed with mean zero and covariance Σ_j^{LF}. Note that the simulation model described in eqs (1 – 3) is for the period 1960 – 2010 ($N_{yrs} = 51$), and the posterior is conditioned on observations which are available for 1980 – 2010, hence N_{Obs} = 31. The likelihood function is therefore a multivariate function of the difference between modeled and observed mole fractions;

$$P\left(D_j\middle|\theta_{11},\theta_{12},\theta_{113}\right) = \frac{1}{\sqrt{(2\pi)^{N_{Obs}}\,|\Sigma_j^{LF}|}}\exp\left(-\frac{1}{2}\boldsymbol{\epsilon}_j^T\left(\Sigma_j^{LF}\right)^{-1}\boldsymbol{\epsilon}_j\right) \quad (9)$$

The covariance matrix, Σ_j^{LF}, represents the sum of the uncertainties of modeled and observed mole fractions. CFC-11 and 12 are both measured to an estimated accuracy of around 1%, and CFC-113 is measured to an accuracy of approximately1.5%[17]. We adopt these values and assume that errors from observations are equivalent to approximately 1% of observed CFC-11 and CFC-12 mole fractions, and 1.5% of observed CFC-113 mole fractions. We do not know the uncertainty of the simulation model, and chose uncertainties for the simulation model component of uncertainty equivalent to 2% of observed mole fractions for CFC-11 and 12, and 4% of observed mole fractions for CFC-113. Taken together and assuming an additive error model, these choices lead to Σ_j^{LF} having diagonal elements equal to $0.03\times D_j$ for CFC-11 and CFC-12, and $0.055\times D_j$ for CFC-113. We assume high autocorrelation in error terms and include autocorrelations

499 in the off-diagonals of 0.99, 0.99 and 0.98 for CFC-11, CFC-12 and CFC-113,
500 respectively. This parameterizes the strong influence of near-fully correlated uncertainties
501 such as scale errors. The selections for uncertainties and autocorrelation values were
502 based on expert judgment. Autocorrelation values as low as 0.95, and uncertainties
503 ranging from 1 to 5.5% were tested and results were within uncertainty of those provided
504 here.
505
506 *Estimating Posteriors*
507 As in Lickley et al. (2020), the posteriors are estimated using the sampling importance
508 ratio (SIR) method, which involves sampling from the priors and then resampling the
509 prior samples based on an importance ratio proportional to the likelihood function (see
510 Bates et al. (2003)[18] and Hong et al. (2005)[19] for more details). Using a sequential
511 updating approach, we implement the sampling procedure twice, first to obtain the
512 posterior $P(\theta_{11}, \theta_{12}, \theta_{113}|D_{11}, D_{12})$ as shown in eq (5). For this iteration of the SIR
513 method, the prior distribution is the joint prior distribution of all three molecules,
514 $P(\theta_{11}, \theta_{12}, \theta_{113})$, as described above. The posterior is then obtained by resampling based on
515 weights proportional to the importance ratio;

$$\frac{P(\theta_{11}, \theta_{12}, \theta_{113}|D_{11}, D_{12})}{P(\theta_{11}, \theta_{12}, \theta_{113})} \propto P(D_{11}|\theta_{11}, \theta_{12}, \theta_{113})P(D_{12}|\theta_{11}, \theta_{12}, \theta_{113}) \quad (10)$$

516
517 The posterior distributions obtained in the first iteration are then treated as the priors in
518 the second updating stage. Note that the only component of θ_{113} that is conditioned on

519 D_{11}, D_{12} are the atmospheric lifetimes. To obtain the full posterior, we resample from the
520 updated priors based on weights proportional to the importance ratio;

$$\frac{P(\theta_{11}, \theta_{12}, \theta_{113}|D_{11}, D_{12}, D_{113})}{P(\theta_{11}, \theta_{12}, \theta_{113}|D_{11}, D_{12})} \propto P(D_{113}|\theta_{11}, \theta_{12}, \theta_{113}). \quad (11)$$

521

522 To sample from the priors, we use a sample size of N = 1,000,000. The first iteration of
523 resampling uses an N= 300,000, and the second iteration of resampling uses an
524 N=100,000. To check the convergence of the SIR algorithm on the true posterior, the
525 BPE was implemented 10 times. The range in estimated values of the median of each
526 lifetime distribution, as well as the 95% and 68% confidence intervals, was within 3%
527 across the 10 iterations of the model, and median values were well within the uncertainty
528 of lifetime estimates reported below.

529

530 **Acknowledgments.** MJL and SS acknowledge the support of VoLo foundation. MJL
531 acknowledges support from the Martin fellowship and SS acknowledges support from the
532 Martin chair.

533

534 **Author Contributions:** All authors conceptualized the work. MJL conducted the
535 analysis. All authors contributed to the interpretation of the data. MJL drafted the
536 manuscript and all authors contributed substantial revisions of the manuscript.

537

538

Data Availability

The datasets generated and/or analysed during the current study are available upon request from M.L (mlickley@mit.edu).

Code Availability

All code used in this work is available upon request from M.L. (mlickley@mit.edu). All analyses were done in MATLAB.

Competing Interests

The authors declare no competing interests.

References

1. Newman, P. A. *et al*. What would have happened to the ozone layer if chlorofluorocarbons (CFCs) had not been regulated? *Atmos*. *Chem*. *Phys*. **9,** 2113–2128 (2009).
2. Solomon, S. *et al*. Emergence of healing in the Antarctic ozone layer. *Science* **353,** 269–274 (2016).
3. WMO: Scientific Assessment of Ozone Depletion. Global Ozone Research and Monitoring Project – Report No. 58. 588 (2018).
4. Montzka, S. A. *et al*. An unexpected and persistent increase in global emissions of ozone-depleting CFC-11. *Nature* **557,** 413 (2018).
5. Rigby, M. *et al*. Increase in CFC-11 emissions from eastern China based on atmospheric observations. *Nature* **569,** 546–550 (2019).

6. Lickley, M. *et al*. Quantifying contributions of chlorofluorocarbon banks to emissions and impacts on the ozone layer and climate. *Nat*. *Commun*. **11(1),** 1-11. (2020).
7. SPARC Report on the Lifetimes of Stratospheric Ozone-Depleting Substances, Their Replacements, and Related Species, M. Ko, P. Newman, S. Reimann, S. Strahan (Eds.), SPARC Report No. 6, WCRP-15/2013.
8. Prather, M. *et al*. in *Climate Change 2001: Scientific Basis: Contribution to Working Group I to the Third Assessment Report of the Intergovernmental Panel on Climate Change* (eds. Houghton, J. T. et al.) 881 (Cambridge University Press, 2001).
9. Chipperfield, M. P. *et al*. Multimodel estimates of atmospheric lifetimes of long-lived ozone-depleting substances: Present and future. *J*. *Geophys*. *Res*. *Atmos*. **119,** 2555–2573 (2014).
10. Rigby, M. *et al*. Re-evaluation of the lifetimes of the major CFCs and Biogeosciences CH 3 CCl 3 using atmospheric trends. *Atmos*. *Chem*. *Phys*. **13,** 2691–2702 (2013).
11. WMO: *Scientific Assessment of Ozone Depletion: 2002, Global Ozone Research and Monitoring Project* – Report No. 47. (World Meteorological Organization, Geneva Switzerland, 2003).
12. Ashford, P., Clodic, D., McCulloch, A. & Kuijpers, L. Emission profiles from the foam and refrigeration sectors comparison with atmospheric concentrations. Part 1: Methodology and data. *Int*. *J*. *Refrig*. **27,** 687–700 (2004).
13. Coordinated & by L. Kuijpers, and D. Verdonik, U. *TEAP (Technology and*

Economic Assessment Panel), Task Force Decision XX/8 Report, Assessment of Alternatives to HCFCs and HFCs and Update of the TEAP 2005 Supplement Report Data. (2009).

14. UNEP. *Decision XXX/3 TEAP Task Force Report on unexpected emissions of Trichlorofluoromethane (CFC-11) - Final Report (Volume 1)*. (2019).

15. Poole, D. & Raftery, A. E. Inference for deterministic simulation models: the Bayesian melding approach. *J. Am. Stat. Assoc*. **95,** 1244–1255 (2000).

16. Daniel, J. S., Velders, G. J. M., Solomon, S., McFarland, M. & Montzka, S. A. Present and future sources and emissions of halocarbons: Toward new constraints. *J. Geophys. Res. Atmos*. **112,** (2007).

17. Engel, A. et al. Update on Ozone-Depleting Substances (ODSs) and other gases of interest to the Montreal Protocol, Chapter 1 in Scientific Assessment of Ozone Depletion: 2018, Global Ozone Research and Monitoring Project - Report No. 58. (World Meteorological Organization, 2019).

18. Bates, S. C., Cullen, A. & Raftery, A. E. Bayesian uncertainty assessment in multicompartment deterministic simulation models for environmental risk assessment. *Environmetrics . J. Int. Environmetrics Soc*. **14,** 355–371 (2003).

19. Hong, B., Strawderman, R. L., Swaney, D. P. & Weinstein, D. A. Bayesian estimation of input parameters of a nitrogen cycle model applied ot a forested reference watershed, Hubbard Brook Watershed Six. *Water Resour. Res*. **41,** W03007 (2005).

Figures

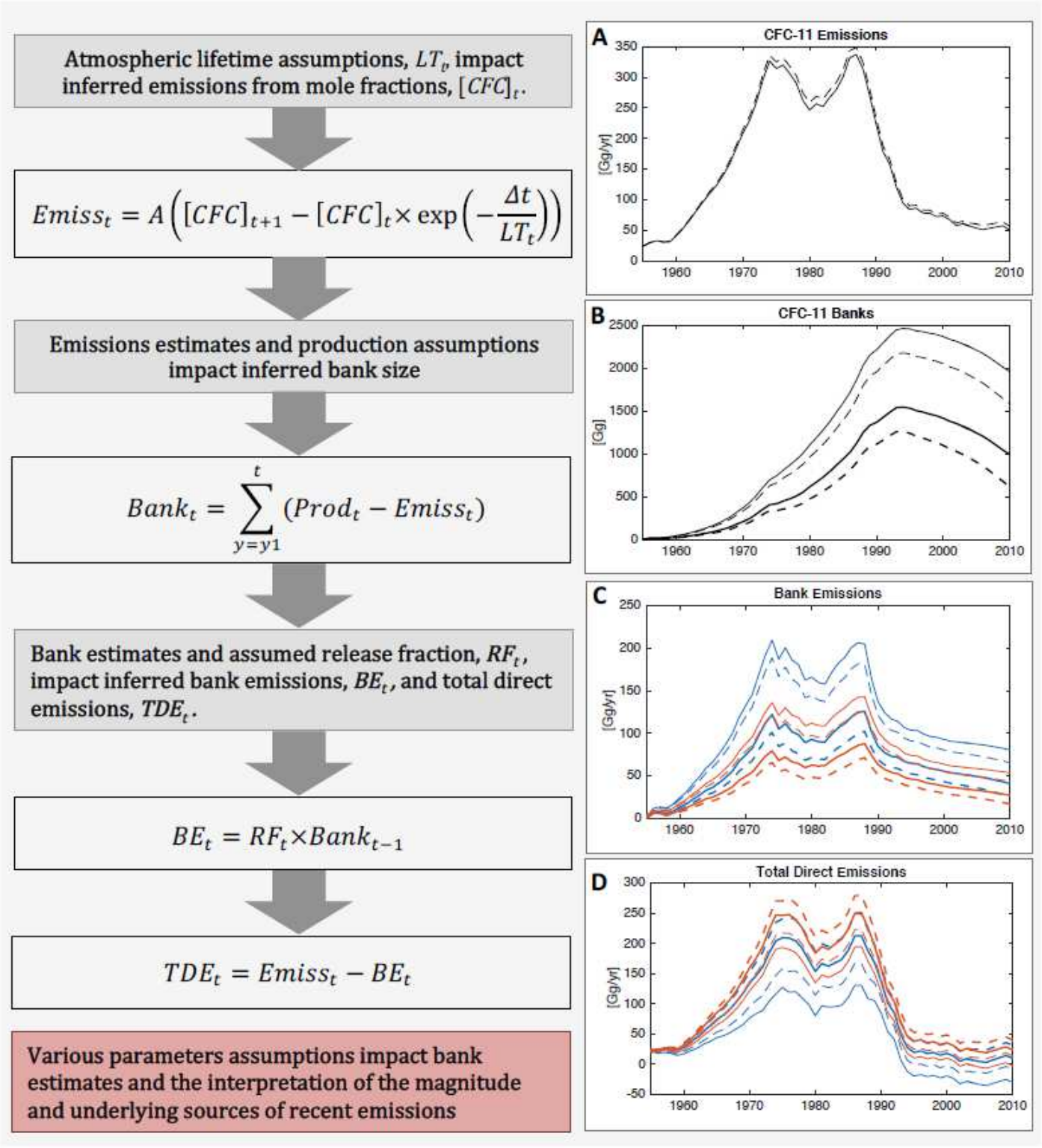

Figure 1

Diagram of the impacts of parameter assumptions including lifetime (LT) on inferred total emissions (Emiss) obtained from observed concentrations, as well as bank size (Bank), bank emissions (RF×Bank) and total direct emissions (TDE). Panel A illustrates the impacts of two lifetime assumptions on inferred

total emissions, while Panels B-D provide illustrative examples to show the sensitivities of the breakdown of sources of those emissions to components from banks versus direct emissions. The solid lines throughout correspond to quantities derived assuming the SPARC multi-model mean time-varying lifetime, and the dashed lines correspond to an assumed constant lifetime of 52 years, adopted as the steady state lifetime in the work of Rigby and colleagues5 and WMO (2018)3. Panel A shows the emissions estimate using the first equation. The parameter, A, is a constant that converts units of atmospheric concentrations to units of emissions. Panel B shows the bank estimates for the two lifetime scenarios and two illustrative production scenarios; bank estimates using reported production are shown using the thicker lines, and the thinner lines correspond to a production scenario that is 10% larger than reported. Panel C shows inferred bank emissions for the lifetime scenarios and production scenarios described above. The colors of the lines indicate different bank release fraction estimates. Blue lines correspond to bank emissions for the median of the prior release fractions distributions used in the analysis from this paper. The red lines correspond to the median +1 of the prior release fraction distribution. Panel D shows the broad range of resulting inferred direct emissions, with the lines corresponding to the same scenarios used in Panel C.

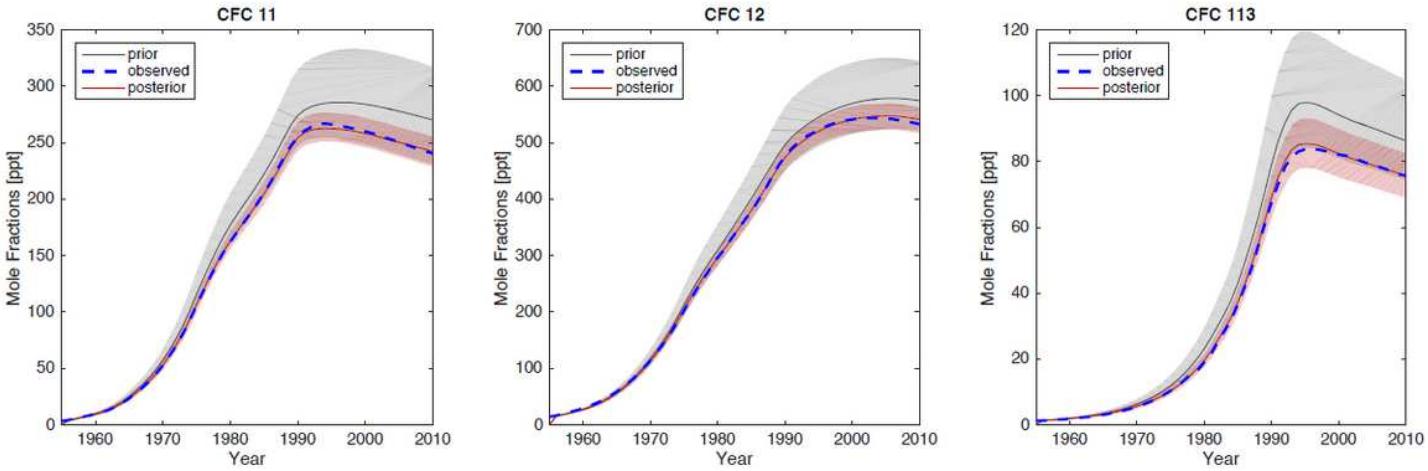

Figure 2

Mole fraction estimates. The grey line and shaded region indicate median and 95% CI of the prior distribution for each molecule. The dashed blue lines are observed concentrations and the red line and shaded region indicate the median and 95% CI for the posterior distributions.

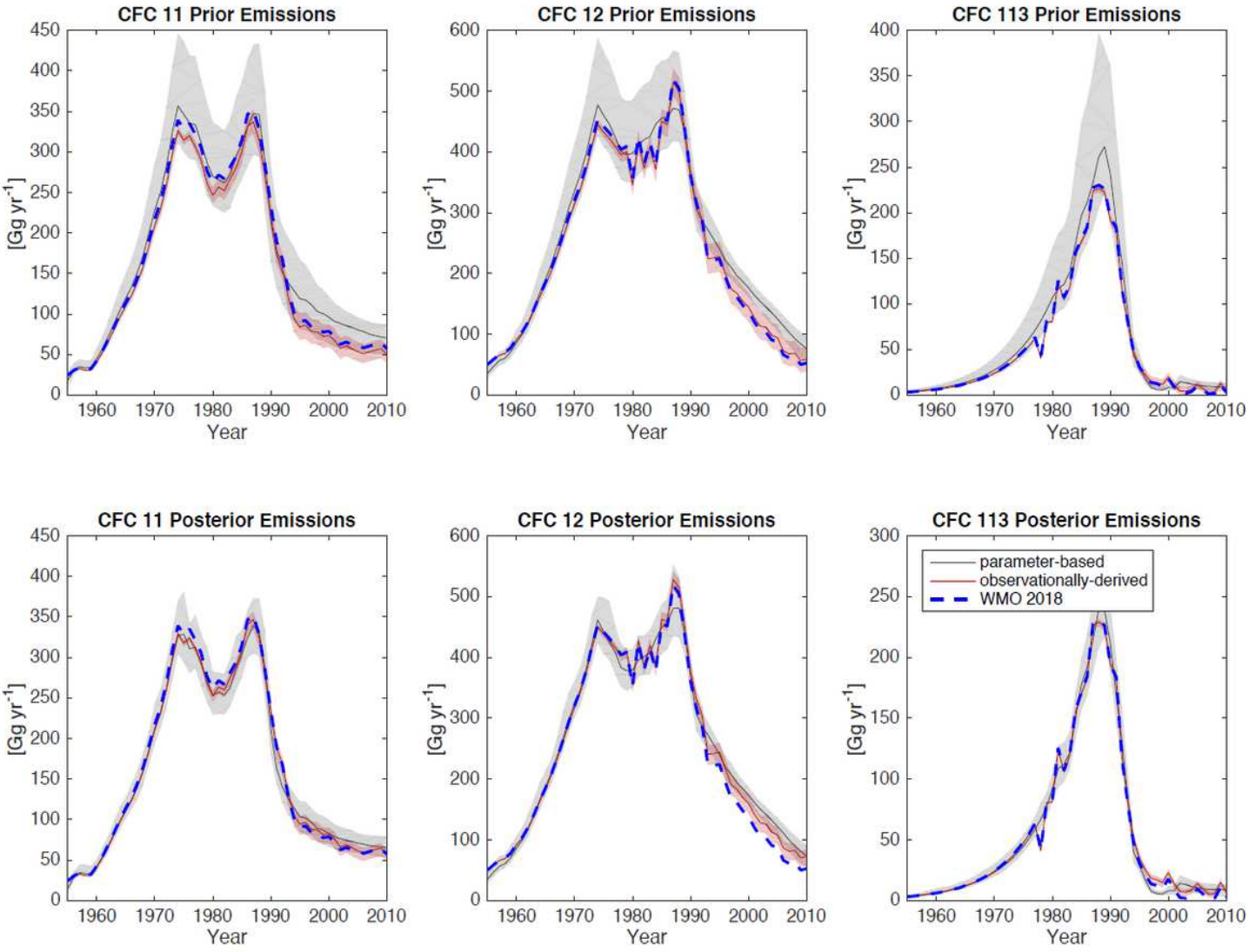

Figure 3

Emissions comparisons of observationally-derived 202 (red) and parameter-based (grey) inferred emissions for the priors (top figures) and posteriors (bottom figures). The solid lines indicate the median and the shaded region indicates the 95% CI for both prior and posterior distributions. The uncertainties in observationally-derived emissions reflect the role of uncertainties in lifetimes and thus are updated in the posterior to reflect the lifetime posterior estimates.

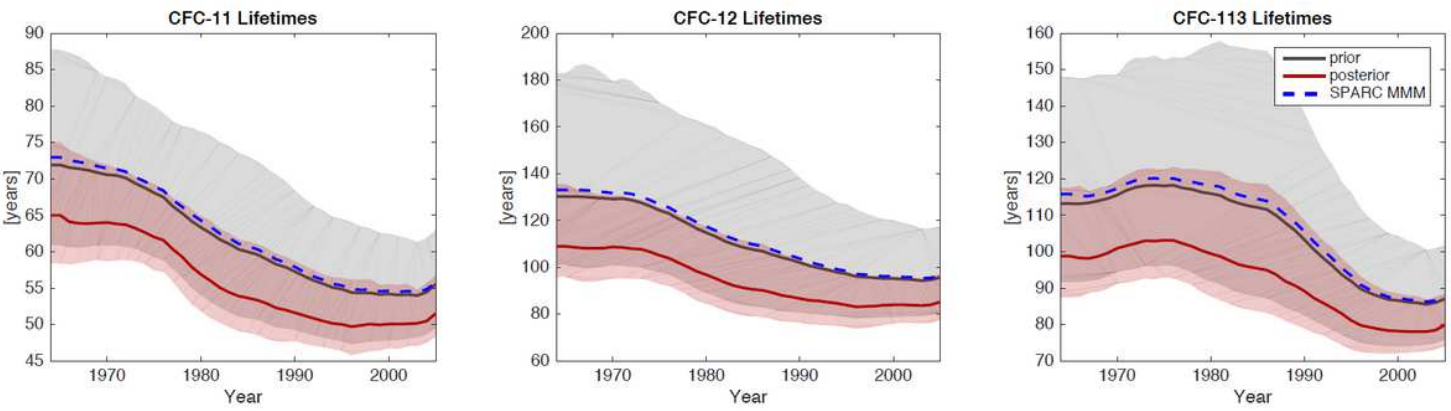

Figure 4

Time varying lifetime distributions. The black line and grey shaded region indicate the median and 95% CI of the prior lifetimes, derived from SPARC modeled values. The dashed blue line indicates the SPARC multi-model mean. The red line and shaded region indicate the median and 95% CI of the posterior lifetime distributions.

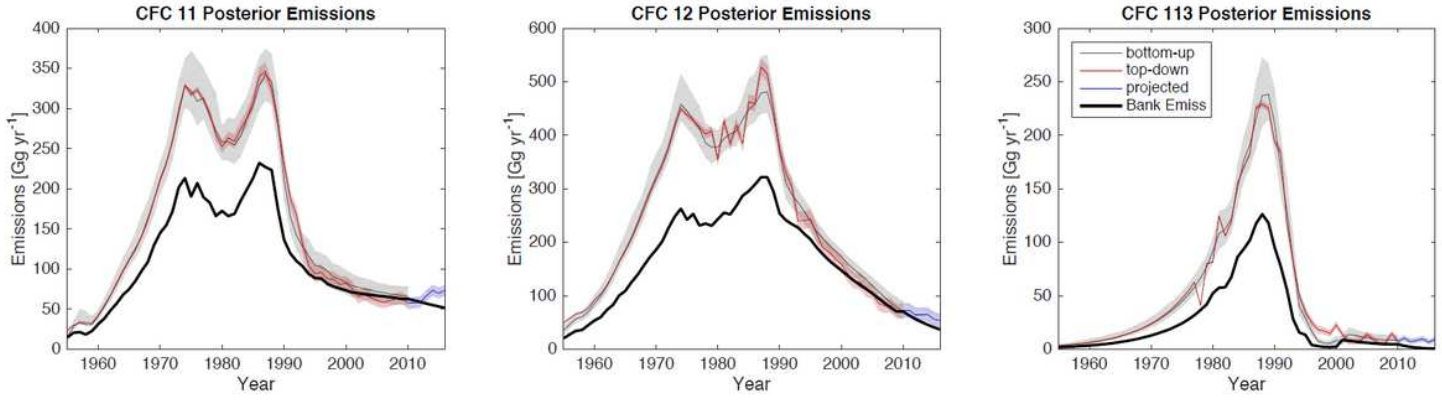

Figure 5

Posterior emissions (red and grey), median posterior bank emissions (black), observationally derived emissions with posterior lifetimes (blue). Shaded regions indicate the 95% confidence interval.

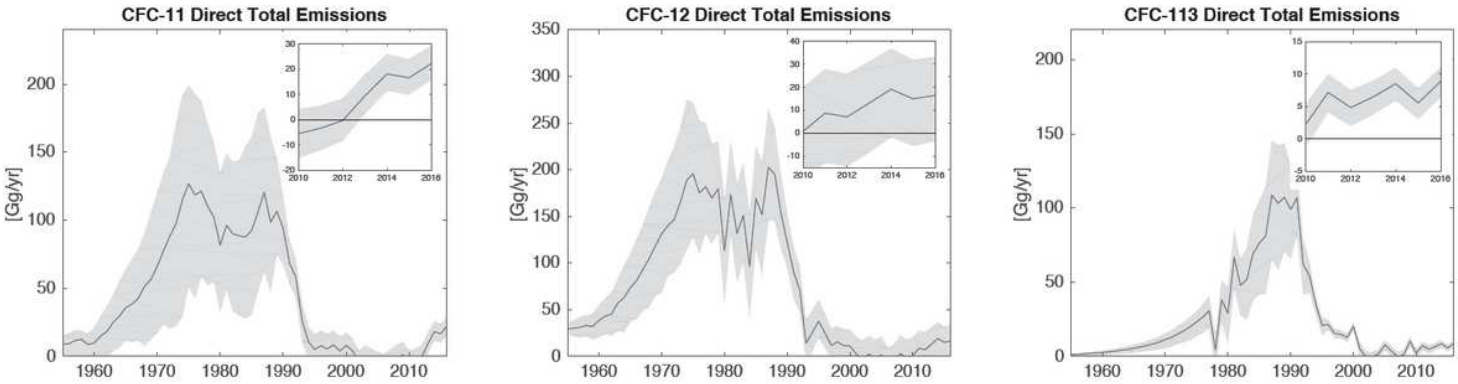

Figure 6

Direct total emissions (i.e. posterior top-down emissions minus bank emissions). Shaded region indicates the 95% confidence interval.

Supplementary Files

This is a list of supplementary files associated with this preprint. Click to download.

- LickleyNatCommssubmission1SupplementaryFigures.pdf